

Commutation Torque Ripple Reduction in Brushless DC Motor Drives Using a Single DC Current Sensor

Chang-hee Won, Kyo-Beum Lee, Dae-Jin Bak, Joong-Ho Song, Ick Choy, Ji-Yoon You*

Intelligent System Control Research Center, KIST, Seoul, Korea
39-1 Hawolgokdong, Seongbukgu, Seoul 136-791, KOREA
jhsong@amadeus.kist.re.kr

* Dept. of Electrical Engineering
Korea University, Seoul, Korea

ABSTRACT - This paper presents a comprehensive study result on reducing commutation torque ripples generated in brushless dc motor drives with only a single dc-link current sensor provided. In brushless dc motor drives with only a single current sensor, the commutation torque ripple suppression that is practically effective in low speed as well as high speed regions has not been reported. A proposed commutation compensation technique based on deadbeat dc-link current controller takes a closed loop control scheme and a parameter insensitive property. The proposed control method is verified through simulations and experiments.

1. Introduction

Brushless DC motor (BLDCM) with trapezoidal counter EMF has been widely used due to its high power density and easy control methodology. Moreover, basic trapezoidal BLDCM can use a single dc-link current sensor to regulate the current flowing through two motor phases. When 120° rectangular stator current control is performed based on a single current sensor as shown in Fig.1, commutation torque ripples usually occur due to the loss of exact phase current control during phase current commutation intervals. The commutation torque ripple in trapezoidal BLDCM typically shows torque spikes in the low speed range and dips in the high speed range. A theoretical analysis related with these commutation torque ripples is found in [1, 2].

Methods for reducing the commutation torque ripple in BLDCM with a single current sensor have been reported in several literatures; to adjust commutation time of inverter switch to control the non-commutation current [2], to overlap switching with a constant duty in off-going phase[3], to apply the effective excitation voltage amplitude[4], to force PWM in on-going phase[5]. However, these conventional methods have limited usefulness in practical applications due to motor parameter sensitivity and dissatisfactory performance over wide speed range.

In this paper, based on a deadbeat current controller, a new torque ripple suppression technique that is insensitive

against machine parameter variation as well as effective all over the wide speed range is developed.

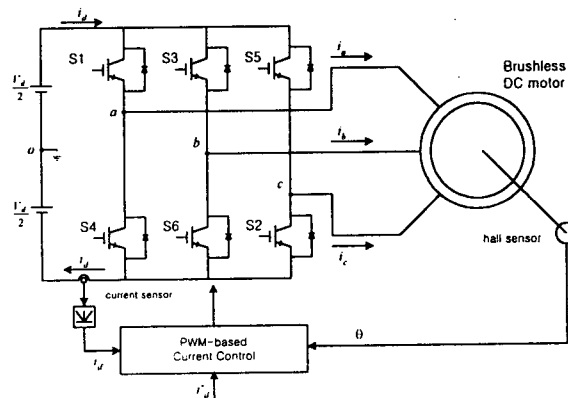


Fig. 1 Basic configuration of trapezoidal brushless DC motor drives with DC link current sensed

2. Current Control

2.1 Normal mode

Fig. 2 shows phase currents, dc-link current, and equivalent circuits when inverter switches S2 and S3 operate in PWM mode. According to on and off conditions of the inverter switches, the voltage equations related with this normal operation mode can be described as

$$v_{bc} = V_d = 2R \cdot i_d + 2L \frac{di_d}{dt} + e_{bc} \quad (1)$$

$$v_{bc} = -V_d = -2R \cdot i_d - 2L \frac{di_d}{dt} + e_{bc} \quad (2)$$

Combining the above two equations by introducing the switching function S, the resultant voltage equation can be rearranged as

$$S \cdot V_d = 2R \cdot |i_d| + 2L \left| \frac{di_d}{dt} \right| + 2E \quad (3)$$

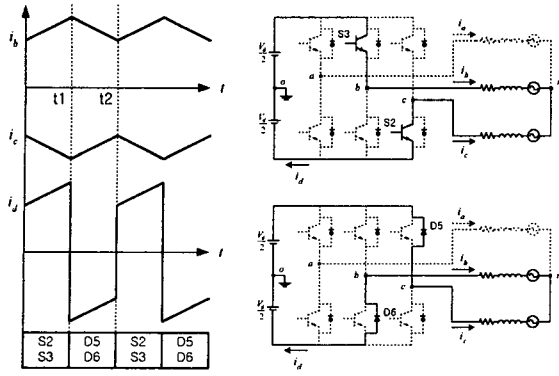


Fig. 2 Normal mode operation

Considering the sign relation of the switching function S and the dc-link current, the following equation is formulated for the deadbeat current controller based on the dc-link current sensor. It is noted that the required information on counter EMF is not the overall waveform but the magnitude value within the flat interval of the counter EMF waveform.

$$V_m^* = K_1 \cdot |i_d(k-1)| + K_2 \cdot (i_d^*(k-1) - |i_d(k-1)|) + 2E(k-1) \quad (4)$$

where, K_1 , K_2 , and T_s denote $2R$, $2L/T_s$ and sampling interval, respectively.

2.2 Commutation mode

When the deadbeat controller in the normal mode is directly used to the commutation mode, the resulting waveforms are shown in Fig. 3. It can be seen in this figure that control of dc-link current cannot be accomplished exactly during commutation interval. Since the dc-link current cannot be tightly controlled close to the current reference value within a sampling interval, T_s , the corresponding terminal voltage reference value V_m^* becomes to be a certain saturation voltage, $V_{m,sat}$. In this mode, deadbeat current controller becomes of no effect. As a result, such a saturation phenomenon of the current controller causes commutation torque ripples during commutation intervals. It is known that spikes and dips imposed on the un-commutated phase current waveform reflect the corresponding commutation torque ripple on the generated torque. This problem can be suppressed by using a commutation compensation technique proposed in the following section.

3. Commutation Torque Ripple Reduction Technique

It is seen in the preceding section that deadbeat current controller is uncontrollable because of the controller

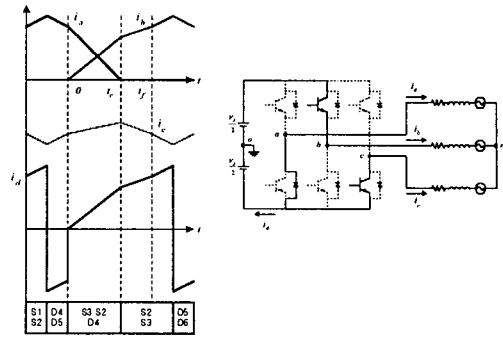


Fig. 3 Commutation mode operation; (a) equivalent circuit and several currents, (b) saturation of deadbeat current controller

saturation during commutation period. In order to resolve the problem, therefore, a control technique to compensate the saturated output signal of controller and balance the slopes of commutated phase currents is proposed in the following section.

3.1 Low speed region ($V_d > 4E$)

Fig.4 shows the switching sequence and the respective phase current waveforms during commutation interval at low speed region. Dotted lines present the phase current waveforms and switching patterns $S1'$, $S2'$, $S3'$ when deadbeat current controller is saturated as referred in the preceding section. Solid lines indicate waveforms in case that PWM is performed at duty ratio D_{low} during commutation interval. The terminal voltage is modulated at duty ratio D_{low} to equalize the slopes of the on-going phase current i_b and the off-going phase current i_c . If the winding resistance is neglected, D_{low} can be calculated as the following equation. Referring to Fig. 4, phase voltage equations during commutation interval can be described as Equations (5)-(7) and the neutral voltage is given by Equation (8).

$$-\frac{V_d}{2} = R \cdot i_a + 2L \frac{di_a}{dt} + e_a + V_{no} \quad (5)$$

$$S \cdot \frac{V_d}{2} = R \cdot i_b + 2L \frac{di_b}{dt} + e_b + V_{no} \quad (6)$$

$$-S \cdot \frac{V_d}{2} = R \cdot i_c + 2L \frac{di_c}{dt} + e_c + V_{no} \quad (7)$$

$$V_{no} = -\frac{V_d}{2} - \frac{e_a + e_b + e_c}{3} \quad (8)$$

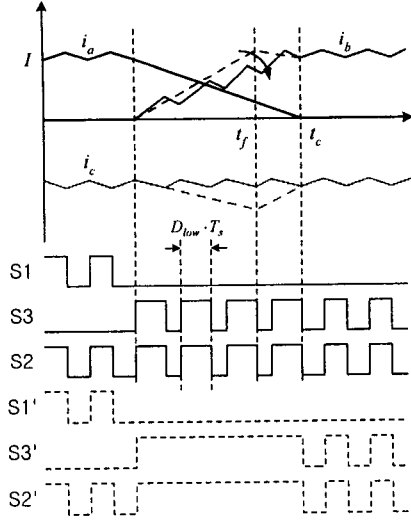


Fig. 4. Switching patterns and commutation in low speed

In this case, phase A current i_a can be described as Equation (12), and commutation time t_c can be defined by Equation (13).

$$i_a(t) = \frac{V_d + 2E}{3L} t + I \quad (9)$$

$$t_c = \frac{3LI}{V_d + 2E} \quad (10)$$

Using the state-space averaged modeling, phase B current can be presented as the following Equation (11). D_{low} that makes i_c come to average current I at time instant t_c can be computed as Equation (12).

$$i_b(t) = \frac{(3D_{low} - 1)V_d - 2E}{3L} t \quad (11)$$

$$D_{low} = \frac{2}{3} + \frac{4E}{3V_d} = \frac{1}{3} \left(2 + \frac{4E}{V_d} \right) \quad (12)$$

3.2 high speed region ($V_d < 4E$)

In high speed region, commutation operation can be described as shown in Fig. 5. In this case, PWM operation is done with only phase A switch S1 to make the off-going phase A current decrease slowly. Similarly, phase B current i_b , phase A current i_a , and duty ratio D_{high} can be given by

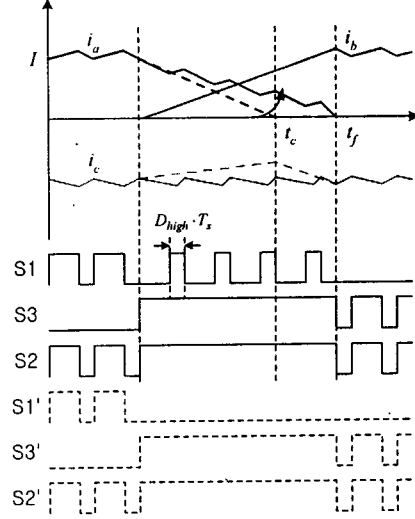


Fig. 5. Switching patterns and commutation in high speed

$$i_b(t) = \frac{(2 - D_{high})V_d - 2E}{3L} t \quad (13)$$

$$i_a(t) = \frac{V_d(2D_{high} - 1) - 2E}{3L} t + I \quad (14)$$

$$D_{high} = \frac{4E}{V_d} - 1 \quad (15)$$

Looking into Equations (12) and (15), the duty ratio of inverter has no relation with the inductance of the motor.

Fig. 6 shows the relation between duty ratio and $4E/V_d$.

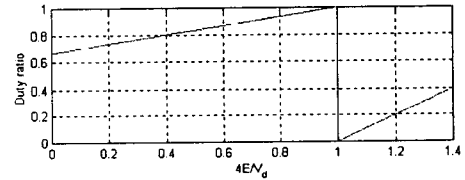


Fig. 6. Duty ratio for commutation compensation

3.3 combination with deadbeat controller

As shown in Fig. 7, the duty ratios derived in the section 3.2 can be combined with deadbeat current controller. Such a deadbeat current controller is designed for compensating saturated output signal of controller.

To avoid this signal saturation and torque ripples, the saturated value $V_{m,sat}$ is compensated by a saturation compensating signal v_{comp} as shown in Fig. 8(a). The saturation compensating signal v_{comp} can be computed by Equation (16) in the low speed range and Equation (17) in the high speed range.

$$v_{comp} = 2V_d(1 - D_{low}) \quad (16)$$

$$v_{comp} = 2V_d \cdot D_{high} \quad (17)$$

Fig. 8(b) illustrates that the compensating signal v_{com} is closely related to the motor counter EMF value. In low

speed range, v_{com} decreases gradually according to the motor speed increase in the low speed region, whereas v_{com} increases rapidly in proportion to the motor speed in the high-speed region. It is seen that v_{com} becomes zero at the motor speed corresponding to $V=4E$.

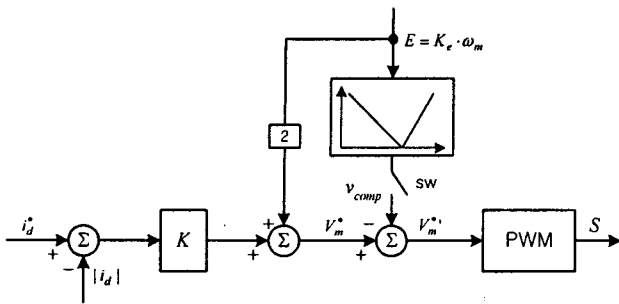


Fig. 7. Deadbeat current controller with commutation compensation

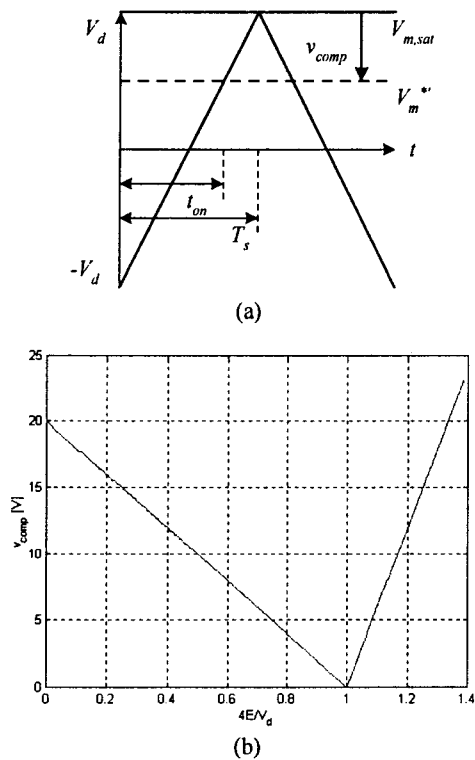


Fig. 8. Commutation compensation level; (a) compensation level calculation, (b) commutation compensation level and counter-emf

4. Simulation and Experiment

To verify feasibility of the proposed algorithm, simulations and experiments are carried out. A PI speed control and commutation compensation loops operate every 50μ s sampling time. Fig. 9 and 10 show simulation

results obtained in the low speed range of 200rpm and in the high speed range of 1200rpm, respectively. It can be shown in these figures that the proposed compensation technique is very effective on the commutation torque ripple suppression. In Fig. 9 and 10, the left-hand side figures show the responses in the case of control scheme without compensation loop, whereas the right-hand side figures show the responses with the compensation loop. Experimental results are shown in Fig. 11 when the motor rotates at 200rpm. Fig. 11(a) shows the phase current ripples generated during commutation when deadbeat controller without commutation compensation is used for current regulation. In Fig. 11(b) where the proposed compensation algorithm is used, the phase current ripples do not appear. Fig. 12 shows the current waveform when the motor rotates at 1200 rpm. It is also shown in Fig. 12 that the current ripples exist when compensation loop is not used, but are reduced when the compensation loop employed.

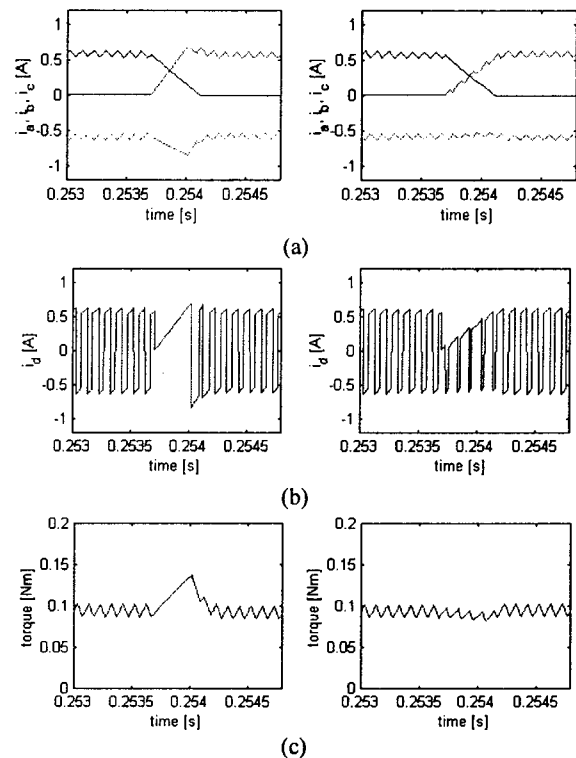


Fig. 9. Simulation results in low speed; (a) phase currents, (b) dc-link current, (c) commutation torque ripple

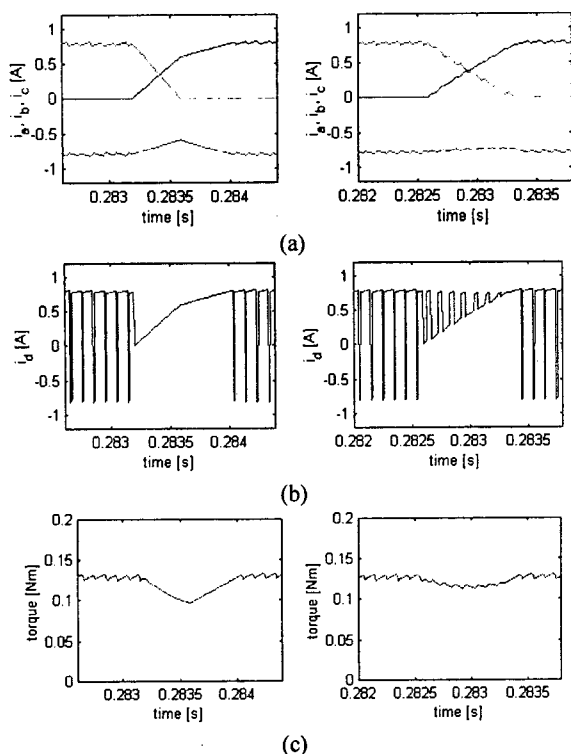


Fig. 10. Simulation results in high speed; (a) phase currents, (b) dc-link current,

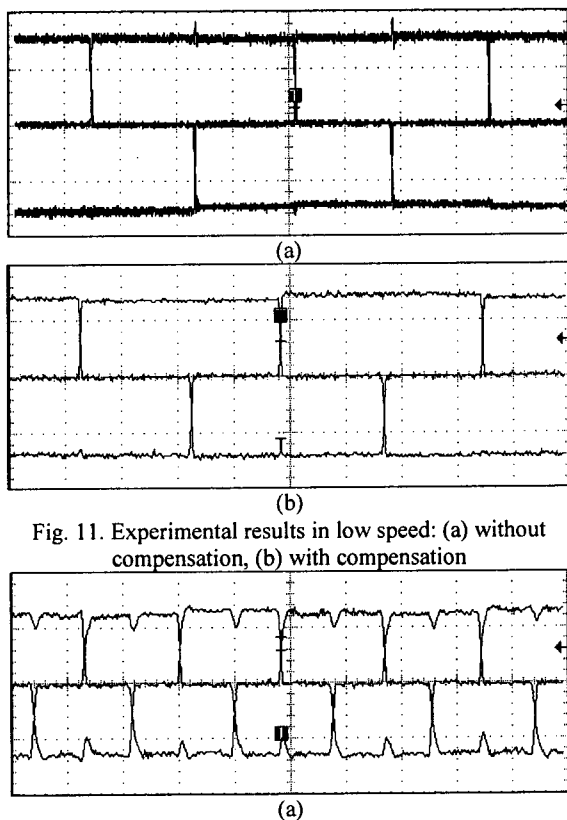


Fig. 11. Experimental results in low speed: (a) without compensation, (b) with compensation

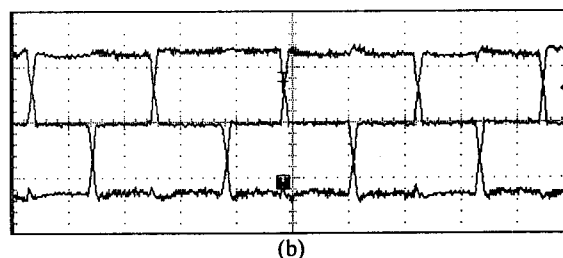


Fig. 12. Experimental results in high speed: (a) without compensation, (b) with compensation

5. Conclusion

In this paper, commutation torque ripples reduction method has been proposed for brushless dc motor drives using a single dc current sensor. In brushless dc drives based on a single dc current sensor, dc-link current sensor cannot give any information corresponding to the motor currents during the line current commutation intervals. Based on the deadbeat current control scheme, the proposed control method aims at suppressing the spikes and dips superimposed on the current and torque responses during the commutation intervals. This scheme gives insensitive characteristics against the system parameter variation and maintains effectiveness in the low speed as well as the high speed regions.

REFERENCES

- [1] T. M. Jahns and W. L. Soong, "Pulsating torque minimization techniques for permanent magnet AC motor drives - a Review," *IEEE Trans. on Industrial Electronics*, vol. 43, no. 2, pp. 321-330, 1996.
- [2] R. Carlson, M. Lajoie-Mazenc, and J. C. S. Fagundes, "Analysis of torque ripple due to phase commutation in brushless dc machines," *IEEE Trans. on Industry Applications*, vol. 28, no. 3, pp.632-638, 1992.
- [3] Y. Murai, Y. Kawase, K. Ohashi, K. Nagatake, and K. Okuyama, "Torque ripple improvement for brushless dc miniature motors," *IEEE Trans. on Industry Applications*, vol. 25, no. 3, pp.441-450, 1989.
- [4] J. Y. Hung and Z. Ding, "Design of currents to reduce torque ripple in brushless permanent magnet motors," *IEE Proceedings-B*, vol. 140, no. 4, pp.260-266, 1993.
- [5] L. Schltting and H-C Skudenly, "A control method for permanent magnet synchronous motors with trapezoidal electromagnetic force " in *proc.EPE*, vol. 4, pp. 117-122, 1991.